AIAA SciTech Forum
23-27 January 2023, National Harbor, MD & Online
AIAA SCITECH 2023 Forum

10.2514/6.2023-1778

Thermite-for-Demise: Preliminary on-Ground Heat Transfer Experimental Testing

F. Maggi[1], A. Finazzi[2], P. Finocchi[3], C. Paravan[4], L. Galfetti[5]
Politecnico di Milano, Milano, MI, 20156, Italy

S. Dossi[6], A. Murgia[7]
ReActive Powder Technology s.r.l., Milano, MI, 20158, Italy

T. Lips[8]
Hyperschall Technologie Göttingen GmbH, Bovenden, 37120, Germany

G. Smet[9], K. Bodjona[9]
ESA/ESTEC, 2200 AG, Noordwijk, The Netherlands

The use of thermite to assist satellite demise is a novel methodology under exploration in the frame of the CleanSpace Initiative of the European Space Agency. The idea consists in inducing an additional heat source during the reentry of a spacecraft, supporting the destruction of those massive components which may not demise completely. Embedding thermites into some components is under investigation within SPADEXO, an ESA-TRP project. One of the key aspects of the energetic component design is the understanding of the best heat transfer mechanism. This paper presents a preliminary on-ground experimental campaign aiming at the quantification of the heat exchanged between a thermite charge and a surrounding metallic structure. This activity aims at demonstrating the capability of spontaneously igniting a thermite charge embedded in a metal vessel subject to external convective flow as well as evaluating the efficiency of the heat transfer process.

I. Nomenclature

C_{316}	=	specific heat of AISI 316
m_c	=	mass of the thermite charge
m_{ce}	=	mass of the thermite charge ejected during test
m_x	=	mass of item x

[1] Associate Professor, Dept. Aerospace Science and Technology, AIAA Senior Member.
[2] PhD student, Dept. Aerospace Science and Technology.
[3] M.Sc. student, Dept. Aerospace Science and Technology.
[4] Assistant Professor, Dept. Aerospace Science and Technology.
[5] Retired Professor, Dept. Aerospace Science and Technology, AIAA Senior Member.
[6] Chief Executive Officer.
[7] Researcher.
[8] Managing Director.
[9] Mechanisms Engineer.

M^i = i-th metal
O = Oxide
P = primer weight fraction
Q_{abs} = Absorbed heat
Q_{th} = Theoretical heat release
T_c = adiabatic flame temperature
x_i = stoichiometric coefficient
Δx = difference of variable "x"
Δt_p = time delay of temperature peak
η = heat transfer efficiency
N.A. = not available

II. Introduction

A. End-of-life of spacecrafts

Management of satellite end-of-life disposal is a problem of paramount importance for sustainable space exploitation. Spacecraft reentry strategy depends on survivability of massive components, being fragmentation a key aspect for on-ground safety of human population. Inside a satellite, some components are more complex to demise than others, due to their geometry and construction material. This is the case of titanium tanks, ball bearing units, and solar array drive mechanisms. When the heat produced during a typical re-entry trajectory is not sufficient and the expected casualty risk overcomes the guideline limit (i.e., 10^{-4} according to the international standard ISO 24113 [1],[2]), a controlled reentry has to be planned and executed. It is generally reported that satellites larger than 500 kg need a commanded demise maneuver, implying a significant additional amount of propellant and, sometimes, the inclusion of dedicated thrusters.

A controlled reentry is an expensive maneuver for a satellite, leading to incremented monetary and mass penalty. It requires a chemical high-thrust propulsion unit and an adequate propellant budget. The use of hybrid architectures (chemical and electric) is also considered. In this latter case, a low-thrust and high-specific-impulse firing lowers the orbit, followed by a high thrust impulse for commanded reentry. A paper by Perrault and co-authors reports the results of a study analyzing different reentry options for a mission, merging 25-year-rule compliance and on-ground casualty risk limit [3]. Within the fences of the work assumptions, the study shows how the increment is mostly affecting the cost of the spacecraft, which can even triple, whereas the expected impact on the mass may be quite limited (below 15 %). For these reasons, in terms of satellite architecture, uncontrolled reentry is generally preferable to controlled reentry. In order to minimize the associated casualty risk, this necessitates Design for Demise (D4D).

In a recent study, Pardini and Anselmo analyzed the reentry of space junk in the time span 2010-2020 (11 years). They found that about 100 tons of uncontrolled large items (cross section wider than 1 m^2) reentered back to the earth, on average, every year and at least one item weighing more than 500 kg reentered every week. Out of the total mass, 21 % was from satellites and the rest from expired rocket bodies. The authors identified that the cumulative risk in that reference period of time was much higher than the guideline threshold, reaching 14 % probability of having a victim [4]. This aspect may become critical when mega constellations are deployed.

The ESA's Annual Space Environment Report 2021 is a clear picture of the status of orbits and spacecrafts [5]. The document demonstrates the progressive achievement of disposal policies. In the 2010-2020 decade, most of small payloads (less than 10 kg) were compliant with the 25-year-rule whereas for payloads smaller than 100 kg the share reduced to about 30-40 %. These satellites are not expected to have a controlled reentry. For larger payloads, a controlled reentry action may be necessary to comply with the ground casualty risk rule. In the category of payloads larger than 1000 kg, the 18 % of the payloads performed a direct reentry in compliance with the 25-year-rule, but not with the casualty risk requirement.

B. Design for Demise (D4D)

When spacecraft reenters Earth's atmosphere, aerodynamic heating associated with high reentry velocities will melt and/or decompose (e.g. through pyrolysis) the spacecraft materials which then ablate. This is the process through which spacecraft demise occurs during Earth reentry. Notably, a dearth of oxygen at high altitudes means that the demise does not involve actual burning of the materials. This is contrary to popular imagery, which often and inaccurately depicts a large fireball.

The demise process and associated mass loss is gradual; therefore, if a spacecraft has sufficiently massive and temperature resistant components, it follows that these may not fully and sufficiently demise during reentry and high energy surviving fragments may reach the Earth's surface and pose an unacceptable casualty risk. In order to mitigate

this risk, the Design for Demise (D4D) paradigm has arisen. This is focused on designing spacecraft components in ways that promote demise during Earth atmosphere reentry. D4D approaches so far have considered the use of alternative materials that are less temperature resistant, modification of component geometries to increase local heat fluxes, embedding of structural weak points to accelerate the spacecraft breakup, containment of multiple surviving fragments to limit their contribution to the casualty risk, and embedding energetic materials within the spacecraft to maximize the available heat for demise. ESA has even published guidelines regarding verification of demise by analysis and testing in support of D4D [6].

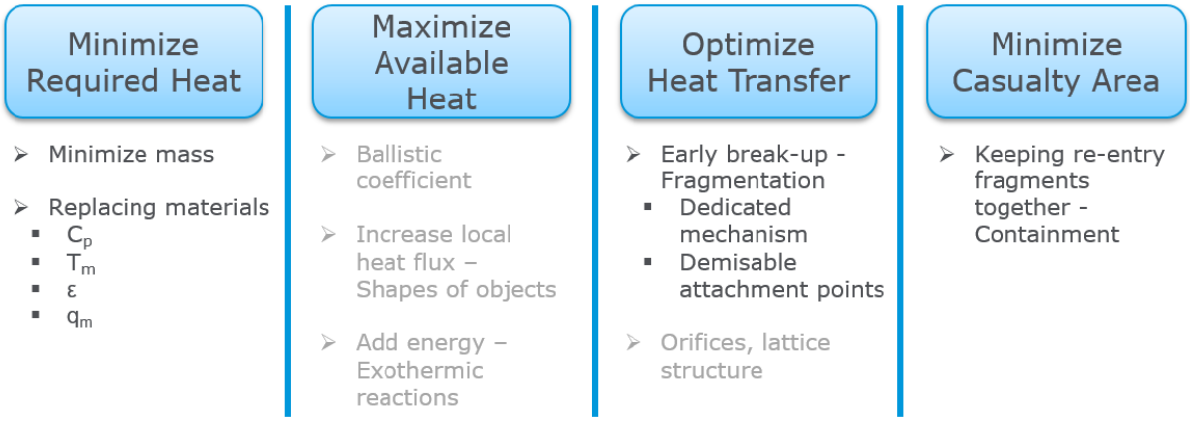

Figure 1: Design for Demise Strategies. The greyed-out entries have not been studied in depth to date.

The various D4D strategies are summarized in Fig. 1. There is currently no consensus over the best approach, however different strategies can potentially be combined. The present study is focused on the second strategy shown, namely maximizing the available heat during reentry. Specifically, this will be achieved through addition of thermite to spacecraft components in what will be called Thermite-for-Demise (T4D).

C. Thermite-for-demise (T4D)

In the case of uncontrolled re-entry, the on-board generation of additional heat, triggered by the natural temperature increase, can contribute to satellite demisability and is one of the new Design-for-Demise (D4D) strategies under consideration [7]. Recent patents proposed the use of space components filled with thermites to support their demise (Refs. [8] and [9]), and experimental tests proved this capability under wind tunnel hypersonic flows [10].

On a satellite, thermites can support demise action with a variety of dedicated strategies [9]. For example, a charge may contribute to the heating of massive undemisable equipment, once embedded in already existing cavities. Specific design adaptations may be required to fully exploit the advantage of thermite contribution. In this case, the reaction is expected to happen in a confined space, favoring energetic compositions characterized by small gas generation to avoid projection of additional debris. On the other hand, severing joints, cables, or interfaces in spacecrafts during demise maneuver may be other possible uses of thermites. These actions may confer variation of shape and aerodynamic features, early exposure of components to reentry heating, or fragmentation of equipment into parts fulfilling the kinetic impact energy thresholds (i.e., less than 15 J). Here, convective heat transfer from an external thermite-filled device (e.g., cutting torch) seems to be the best method. Finally, thermites may be used to create localized thermal stresses in refractory materials. During reentry, ceramic components are difficult to demise because of their high heat resistance, but they are characterized typically by high fragility. Localized heat addition or transfer may be used to induce thermal stresses leading to cracks and fragmentation.

Thermites are powders made by a mixture of a metal and an oxide. These pyrotechnic compositions are characterized by high energy density. Thermophysical properties of products depend on the selected metal/oxide couple. For example, a typical hematite (iron oxide) / aluminum mixture can supply about 4 MJ / kg with a reaction temperature above 3000 K and limited gas production [11]. At the same time, the reactivity of the powder depends on the nature of the ingredients, on the physical properties of the virgin powders (e.g., size, shape), and on the preparation of the mixture. Recently, in the frame of SPADEXO, a Technology Research Program (TRP) of the European Space Agency (ESA), the use of thermites for satellite demise is under investigation. The activity consists in understanding the best strategy to include this additional source of energy inside the demise sequence of a satellite with massive components. The amount of energy added by thermite is modest when compared to the energy generated by the reentry

itself, but a large benefit of T4D is that the energy can theoretically be released where it is most needed and when it is most impactful. However, the timing of ignition cannot rely on a commanded fuse, as the satellite may not be collaborative at that moment of the mission. Reaction triggering must depend on the temperature history generated by the environment on the charge and its envelope.

At this early stage of development there is not yet a clear indication of the best strategy to demise a component with the aid of thermites. The heat transfer mechanism generated by the enthalpy release of the metal/oxide reaction has to be characterized [12]. Hot glowing solid reaction products tend to bear conductive and radiative heat transfer, whereas convection stem from the generated gaseous fraction. General considerations suggest to use a convection-driven mechanism for a torch-kind application, as in Ref. [13], whereas conduction/radiation seem more convenient for an enclosed solution, given the low heat transfer efficiency found in past v-notch experiments by Crane and co-authors (around 10 %) [12].

The present paper describes a test campaign for the quantification of the heat transfer contributions from a charge lodged inside a closed vessel towards a metal enclosure. The experiments are performed at sea level conditions and consist in the thermal monitoring of a cylindrical container embedding small samples of different thermites. After an initial state-of-the-art analysis in Section III, the experimental campaign is described in Section IV. Results on thermites are discussed in Section V whereas discussion and conclusions are drawn in Section VI and VII, respectively.

III. Background

D. Thermites

Thermites are pyrotechnic formulations typically based on metal/metal oxide combinations. The thermite reaction is a redox reaction producing an oxygen transfer between the (starting) oxide (i.e., the oxidizing species source) and the (starting) metal fuel. In case of a metal (M^1) oxidized by a metal oxide ($M^2_{x2}\ O_{x3}$) to generate another metal oxide ($\mathrm{M^1_{x4}\ O_{x5}}$) and a metal ($M^2$), a thermite reaction can be generally represented by the reaction reported in Eq (1) [14].

$$M^1 + \frac{x_5}{x_3\ x_4} M^2_{x2}\ O_{x3} \rightarrow \frac{1}{x_4} M^1_{x4}\ O_{x5} + \frac{x_2 x_5}{x_3\ x_4} M^2 \tag{1}$$

Temperature stability of oxidizing species plays a crucial role in the thermite reaction. Thermodynamics governs the spontaneity of the thermite reaction, prescribing a negative Gibbs free energy balance between reactants and products. This balance can be addressed using the Ellingham diagram [15]. In a similar manner, thermodynamics and stoichiometry determine the ideal behavior of the reaction, including enthalpy of reaction and combustion products (e.g. ideal fraction of evolved gas). The theoretical maximum density (TMD) can be derived from the physical properties of the components and their ratio. In this respect, a comprehensive database is found in a conference paper by Frisher and Grubelich from the Sandia National Laboratories [11]. A small extract is reported in Table 1.

Experimental characterization is mandatory for proper quantification of combustion parameters. Results obtained from every thermodynamic code (e.g., NASA-CEA, RPA, Propep) are implicitly assuming infinite reaction rate and complete efficiency, unless specific losses are explicitly formalized [16]. In real conditions we can assist to derating of ideal performance due to partial reactions, enthalpy loss caused by gas phase escape and heat dispersion, and entrainment of particles by the gas products outside the reaction region [17]. Convection and conduction are the driving heat transfer mechanisms for the combustion wave propagation in thermites. Their rate of reaction (i.e., the propagation speed of the combustion wave after ignition) as well as their ignition properties mainly depend on composition, particle size, oxidizer to fuel ratio, and compaction (i.e., loose powder vs. pressed pellets). The generation of gaseous combustion products has been observed to facilitate faster reaction rates [18]. Also, finer reactants size typically provide faster combustion rates and shorter ignition times because of the larger specific surface area. In this respect, nano-sized Al shows attractive performance but also high sensitivity [19].

Table 1 Thermophysical properties of some thermite reactions. Data are reported per mole of reacted aluminum [11]

Oxide	ΔH_0 per Al mole	ΔH_0 per kg of reactants	T_C	Gas production
Fe_2O_3	$-425.6\ \frac{kJ}{mol_{Al}}$	$-3856.6\ \frac{kJ}{kg}$	3135.3 K	Minor amount of gaseous Fe
CuO	$-603.9\ \frac{kJ}{mol_{Al}}$	$-1594.7\ \frac{kJ}{kg}$	2837.2 K	Relevant fraction of gaseous Cu
Bi_2O_3	$-550.9\ \frac{kJ}{mol_{Al}}$	N.Av.	N.Av.	N.Av.
MoO_3	$-465.3\ \frac{kJ}{mol_{Al}}$	$-3761.3\ \frac{kJ}{kg}$	3812.6 K	Small traces of gasses
SnO_2	$-404.6\ \frac{kJ}{mol_{Al}}$	$-3093.3\ \frac{kJ}{kg}$	3135.3 K	N.Av.

E. Mechanical activation

Activation is a family of methods to process a powder and change some of its original features (namely, shape, microstructure, composition, or surface finishing). The process can also confer the original powder some special feature. The outcomes of the activation process depend on initial ingredients and manufacturing details (e.g., augmented reactivity, catalysis, ease of handling, etc.). There are three main categories of activation: mechanical, chemical, and mechano-chemical. A review can be found in Refs. [20] and [21].

The mechanical activation, used in this work to produce thermites with enhanced reactivity, processes the virgin powder and, if present, the additives with ball milling, grinding the ingredients through a low or a high-energy mill. The process is controlled by the sphere-powder-sphere and/or the sphere-powder-jar wall interactions [21],[22].

Mechanically-activated thermites, also called Mechanically Activated Energetic Composites (MAECs) can be produced by high energy ball milling. By opportunely tuning different process parameters (such as ball milling time and quantity and type of process control agent) it is possible to obtain strong increments of thermites reactivity, beyond the classical ones. The new material offers similar performance with respect to the nanometric counterpart, although maintaining the micrometric size of the components.

IV. Experimental campaign

A. Scope of the experimental investigation

The experimental campaign aims at measuring the fraction of enthalpy released by a thermite charge lodged in the bottom of a metallic container and transferred to the surrounding structure. Two different sets of experiments have been implemented and performed. The first one considers an open vessel containing a thermite charge with ignition provided by a hot wire. The objective of this experiment is to quantify the efficiency of the heat transfer in a configuration where the reactive powder may be ejected from the container. Moreover, this experiment has been used to verify the ignitability of the selected mixtures and to shortlist the energetic materials for the experimental follow-up. The second set of experiments considers a closed geometry. The reaction is obtained by heating the vessel where the thermite has been sealed to ignition temperature, with a hot air blower. Some thermite pressed pellets have been introduced in the formulation. This second configuration aims at measuring the heat transfer efficiency in a condition that prevents reactive components to be entrained by reaction products and at verifying the ignition behavior of the energetic material, confined in a vessel heated up only through convection, without exposing directly the thermite to the heat source.

B. Experimental setup

1. Open-barrel configuration

The thermite charge is lodged in a hollow cylinder with an internal diameter of 9.1 mm, a thickness of 2.3 mm and a height of 100 mm. This barrel is made in AISI 316L, which is an austenitic stainless steel widely used in aerospace industries, thanks to its favorable thermal properties and great resistance to corrosion in a reducing environment. This

metallic cylinder is externally threaded for a length of about 10 mm on each side and can be coupled with caps. The vessel is up-ended. In this configuration, only one cap seals the base of the cylinder, creating the thermite lodging and preventing the spillage of solid and gaseous combustion products from the bottom. The thermite charge is triggered by means of an electric FeCrAl wire (Kanthal A1), connected to a voltage generator and heated up by Joule effect. Finally, the metallic barrel is externally covered by an insulation layer composed by mineral-wool, having thickness of about 4 mm.

The temperature detection system comprises two N-type thermocouples. The first one is placed at half height of the lower cap, while the other one is adjacent to the external surface of the barrel, at 4 centimeters from the cap. Both thermocouples are taken in place through a layer of Boron Nitride thermal paste. The use of this material is intended to optimize the thermal contact between the thermocouple joint and the metallic substrate to enhance the accuracy of the measurement. The signal is collected by a Pico Technology TC-08 datalogger.

The scheme of the apparatus is visible in Figure 2 whereas Figure 3 is capturing a moment during the application of the insulation (front and side views), right before the covering of the thermocouples and the application of the thermal paste.

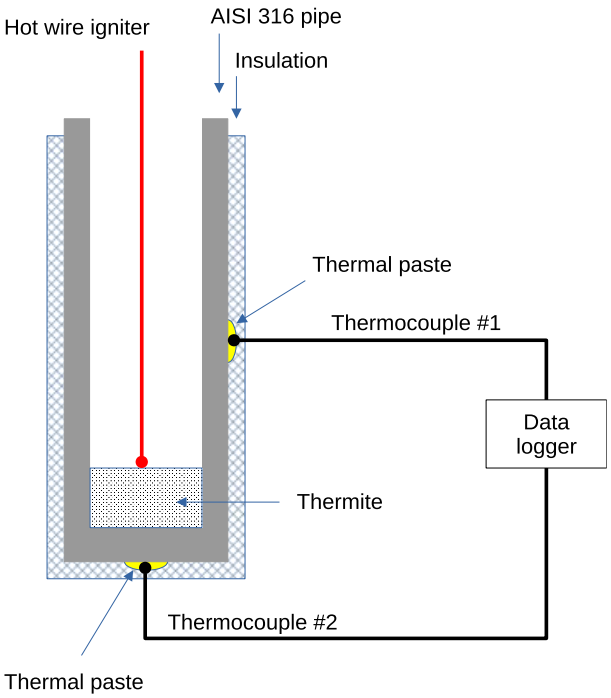

Figure 2 Scheme of the test apparatus for thermite heat transfer test in cylindrical geometry

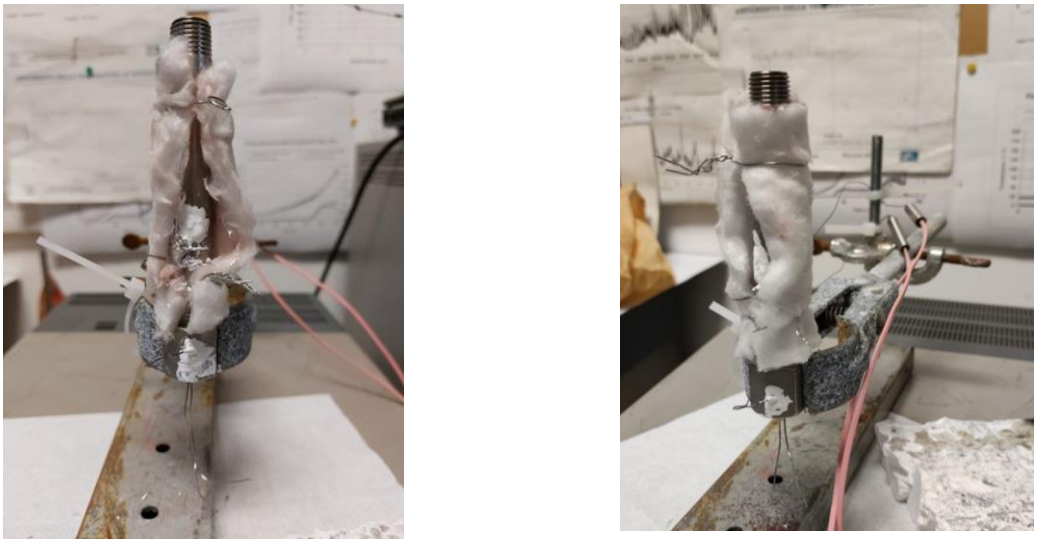

Front **Side**

Figure 3 Open-barrel configuration. Apparatus during the preparation of the test

2. Closed-barrel configuration

In this second configuration the upper cap was applied to the vessel, still in upright position, creating a sealed reaction environment (Figure 4). A convective heat source (Leister Hotwind hot air blower) was placed in front of the closed barrel, as close as possible to its surface (around 1 cm distance). The temperature range of the hot air blower is limited to 900 °C. For this reason, the lower cap was placed in line with the axis of the blower outlet, exposing to the maximum heat flux the enclosure where the thermite is settling. A brass shield was also used to improve the heating. For the same reason, the mineral-wool insulative layer used in the previous set of experiments, was removed.

As in the open-barrel configuration, a set of N-type thermocouples was used to record the thermal history of the container. Three thermocouples have been employed, each one placed at half height of the corresponding element. The Boron Nitride paste is used to enhance the thermal contact with the substrate and to keep the thermocouple in place. A FeCrAl wire was tightened around each component, over the thermal paste, to make the thermocouple placement more robust. A Pico Technology TC-08 datalogger was used for data recording.

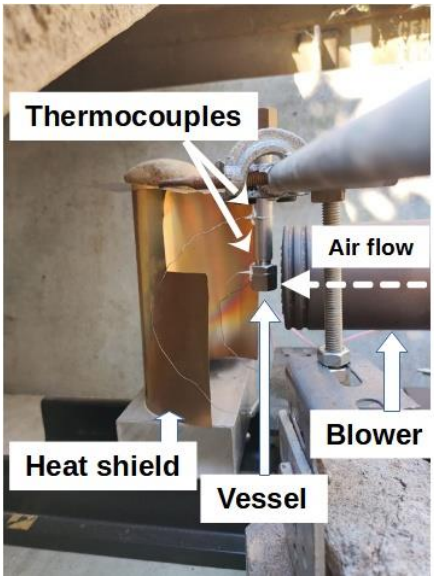

Figure 4: Closed-barrel configuration.

3. Powder characteristics

The thermite formulations used in the experimental campaign, for both open and closed barrel configurations, were obtained by mixing or activating the powders listed in Table 2. In the next sections, standard micrometric powders have been indicated with the symbol "µm", while mechanically activated ones by "ActT".

In all the tests performed, the reactive element is composed by two parts: the main charge, made by an Al+Fe_2O_3 mechanical mix in stoichiometric ratio, and a primer, which triggers the reaction igniting the whole powder. This last fraction needs higher reactivity than the rest of the blend and is produced by mechanical activation. The primer was used either in loose or pelletized form. The ratio P between primer and total charge mass is indicated in Table 3 and Table 4.

Table 2: Characteristics of initial powders.

Species	Nominal diameter, µm	Morphology
Al	30	Spherical
Fe_2O_3	0.4	Spherical
MoO_2	$N.A.$	Spherical

V. Results

A. Open-barrel configuration

Figure 5 shows an example of the temperature traces recorded during the open-barrel tests. The hot wire causes a sudden ignition of the charge. A strong peak running from ambient temperature to about 220 °C is observed by the thermocouple placed on the cap, where thermite is lodged (TC#2, red curve). The barrel temperature (TC#1, green curve) rises at a slower pace, reaching about 80 °C. At the instant of ignition, both charge and vessel were at ambient temperature.

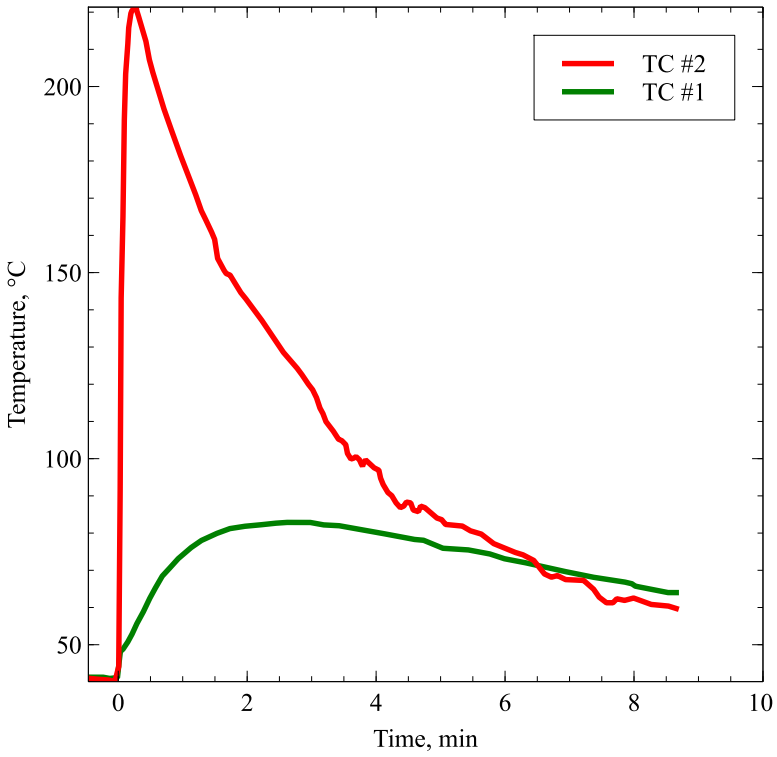

Figure 5: Temperature traces recorded in one thermite ignition test, open configuration. TC #1 is placed on the barrel, TC #2 on the cap containing the thermite.

In order to quantify the heat transfer efficiency from the reacting thermite and the containing structure, the heat absorbed by the steel vessel Q_{abs} is computed as Eq. 1 reports, considering only the enthalpy accumulation in the metal bulk. Losses by convection and radiation are currently neglected making the analysis conservative.

$$Q_{abs} = m_{cap} C_{316} \Delta T_{cap} + m_{bar} C_{316} \Delta T_{bar} \quad (1)$$

In the formula, C_{316} is the specific heat of AISI 316L steel, assumed constant, m_{cap} and m_{bar} are respectively the cap and the barrel masses, and ΔT_{cap} and ΔT_{bar} are the temperature differences experienced respectively by the cap and the barrel, measured between the one recorded at the instant in which the cap reaches its maximum temperature and the one at ignition time. The computed Q_{abs} is then compared to the theoretical heat release Q_{th} and their ratio is named heat transfer efficiency, indicated by the symbol η. For each charge, the initial mass m_c and an estimate of the ejected material during the test m_{ce} are also recorded. Composition list as well as results are indicated in Table 3.

Table 3: Used compositions and obtained results for the open-barrel tests.

Primer oxidizer	P	m_c, g	$\frac{m_{ce}}{m_c}$	Q_{th}, J	Q_{abs} , J	η
Fe_2O_3	16.7 %	1.2	2.08 %	4744.7	3435.4	72.4 %
	16.7 %	1.1	28.2 %	4448.1	2250.9	50.6 %
	24.8 %	1.4	65.4 %	5337.7	2018.9	37.8 %
MoO_2	24.8 %	1.0	4.5 %	4023.8	2070.5	51.5 %
	24.8 %	1.3	19.2 %	4862.7	2774.9	57.1 %

Two activated thermites have been tested as primers in the open-barrel test, one based on iron oxide and one on molybdenum oxide. All powders were in loose form and were mixed with the main thermite charge. An unexpected outcome of this first set of the experiments was the detection of a light green product on a protection bucket used during the tests with thermites based on MoO_2. Being all the main reagents and expected products of a different color, the product has been identified as MoO_3, a suspected carcinogenic agent. Further analyses are necessary to confirm this initial attribution. However, since non-toxicity was one of the selection requirements, as a precautionary measure the tests in closed configuration were performed using only Al+Fe_2O_3 mixtures. Figure 6 shows the evidence of this outcome.

Figure 6: On the left, light green traces on the protective bucket used for open-barrel tests with MoO_2. On the right, MoO_3 powder.

B. Closed-barrel configuration

Figure 7 reports the temperature traces for an experiment carried out in the closed configuration (test 6, Table 4). The hot blower curve (violet) is the temperature detected by a control thermocouple placed in front of the air flow before the barrel. The curve shows a slow heat transient, imposed by the limitations of the convective heat source. The other three curves are showing the temperature evolution of the lower cap (green-blue), the barrel (yellow-red), and the top cap (cyan-brown). Because of the sample mounting, the lower cap is directly exposed to the heat flow of the blower, and, in fact, its thermocouple records the highest temperatures, followed by the one monitoring the tube and, finally, by the curve of the upper cap. The ignition of the charge is clearly visible at about 450 s from the beginning of the test. Both ends of the barrel record the most relevant temperature increase (about 150-200 °C), with the bottom cap developing the rising thermal profile much faster than the upper one. The barrel records a reduced temperature increment, of about 50 °C.

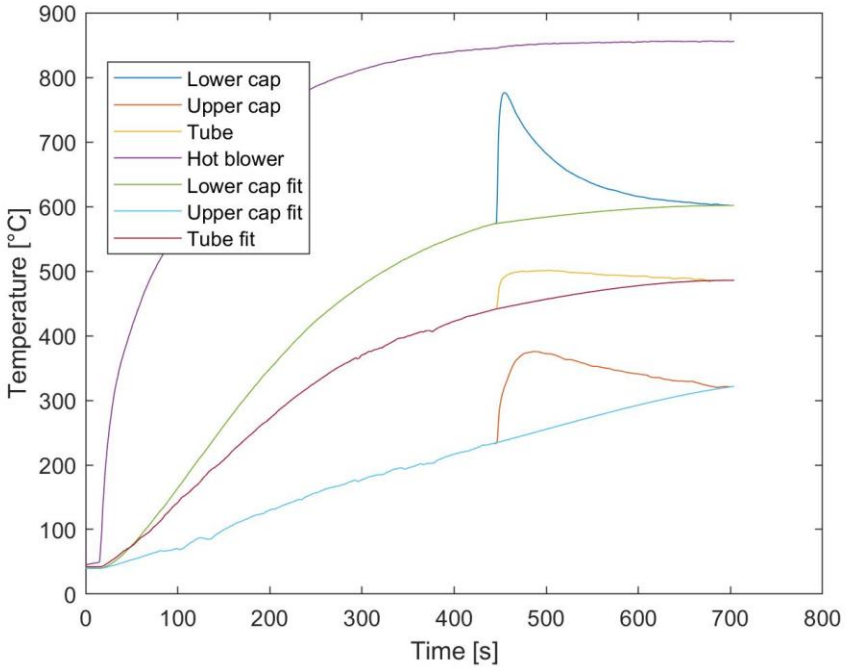

Figure 7: Temperature traces recorded in one thermite ignition test, closed configuration. Numerical fits are used to highlight the expected temperature traces without considering the thermite contribution.

In this configuration, the ignition is provoked by progressive heating of the barrel via the convective external source so it is important to remove the continuative blower contribution from the heat balance, also during the charge reaction. It is not possible to create a set of baseline temperature curves by simply running a heating cycle without thermite reaction because the placement of the barrel in the flow of the blower as well as a sudden variation of external environmental conditions are source of uncertainty that prevent from the derivation of a precise correction curve. For this reason, the baseline curves were rebuilt using numerical fits.

The top cap is also present so now Eq. (2) contains three heat sink terms.

$$Q_{abs} = m_{l,cap} C_{316} \Delta T_{l,cap} + m_{bar} C_{316} \Delta T_{bar} + m_{u,cap} C_{316} \Delta T_{u,cap} \quad (2)$$

Where the subscript "l,cap" stands for the lower cap, while "u,cap" for the upper cap. To achieve a better representation of the heat transfer efficiency, in this case the temperature rise for the component x, marked as ΔT_x, is defined by Eq. (3).

$$\Delta T_x = T_{max,x} - T_{fit,x} \quad (3)$$

$\Delta T_{max,x}$ is the temperature reached by the component x when the lower cap is at its maximum temperature, while $\Delta T_{fit,x}$ is the temperature predicted by the numerical fit for the baseline curve, always for the same component and at the same instant of time. Similarly, the specific heat values are the average between the values reported in Ref. [23] for the same temperature range. Then, the heat transfer efficiency η is computed as the ratio between the one absorbed by the vessel Q_{abs} and the theoretical one released by the thermite Q_{th}.

Tested thermites were based on iron oxide. The main charge was composed by a standard micrometric aluminum/hematite mechanical mix and was always used in loose powder form. The activated primer was tested both in loose and pellet format.

Table 4: Used formulations and obtained results for closed configuration. All tests involve Al+Fe_2O_3 thermite.

Identifier	m_c, g	Type	Configuration	Δt_p , s	Q_{th} , J	Q_{abs} , J	η
1	1 0.5	μ ActT	Loose Loose	10	5937.3	3006.0	50.6 %
2	0.66 0.44	μ ActT	Loose Loose	5	4314.4	3190.0	73.9 %
3	1 0.5	μ ActT	Loose Loose	6	5937.3	3763.5	63.4 %
4	1 0.6	μ ActT	Loose Pellet	14	6333.1	3551.1	56.1 %
5	1 0.6	μ ActT	Loose Pellet	19	6333.1	4193.5	66.2 %
6	2.3 0.6	μ ActT	Loose Pellet	10	11479	5787.9	50.4 %

VI. Discussion

A. Open-barrel configuration

The plot reported in Figure 5 shows two temperature traces recorded by the data logger during a test characterized by a thermite based on micrometric aluminum and a blend of iron oxide and molybdenum oxide. The total thermite amount was 1.2 grams. The green curve reports the signal recorded by Thermocouple #1 (side) and the red curve is the cap temperature (Thermocouple #2).

The peak of curve #2 is quite pronounced and the rise is steep, meaning that the thermite is reacting quite violently. The steepness of the peak suggests that most of the heat transfer is caused by conduction/radiation within the cap. Despite part of the material was projected outside the barrel, the temperature of the cap rose by about 180 K. The green curve (#1) shows that the side temperature grows much slower and it takes some minutes to reach the peak value. In this latter case the delay is probably caused by the heat transfer from the cap to the barrel body, with only a minor contribution attributed to convection during the firing time. All the registered temperature traces show a similar behavior.

Table 3 reports an overview of the outcomes of the open-barrel tests. Even if efficiency data are quite variable, spanning from 37.8 % to 72.4 %, all the values are significantly higher than the ones reported in the literature (about 10 %) [12]. The improved confinement, despite the opening at the upper end of the barrel, seems to be a key factor to determine the efficiency of the heat transfer. An element that strengthens this hypothesis is the trend that can be observed for the iron oxide thermite: the higher the fraction of ejected products, the lower the heat transfer towards the container structure. The higher heat transfer (72.4 %) corresponds to a very low ejected mass (2.08 %), while a significant increase in the mass loss (up to 65.4 %) reflects a decrease in heat transfer of about a factor 2 (to 37.8 %). The tests performed using MoO_2 show a limited variation in mass loss and in heat transfer efficiency. This could indicate that either the Al+MoO_2 combustion depends on a less variable heat transfer efficiency, or that a difference of 15 % in the mass loss is not so impactful on η, which has an average value of 53.9 %.

B. Closed-barrel configuration

Figure 7 reports an example of the temperature traces registered for the closed-barrel configuration ignition tests. Again, the temperature increase due to the ignition of the thermite charge is clearly detectable in traces monitoring the container. An interesting characteristic of the traces is that the temperature slope decreases with the distance of the considered component from the thermite charge. This is probably because the upper cap, for example, receives heat mainly by conduction from the other components or radiation from the reaction products, and not by convection, given the quick reaction of the thermite.

Despite some fluctuation in the heat transfer efficiency, the elimination of the mass ejection seems to limit losses and variability. Whereas in the open configuration tests a value as low as 37.8 % was reached, for the closed configuration the lowest efficiency is about 50 %, within a narrower experimental range. The variation appears to be independent from the way the activated thermite primer was assembled in the vessel. Pelletized and loose powders performed in a similar manner with an average efficiency value of about 60 %, higher with respect to the open-barrel result.

Even if it was not possible to directly measure the combustion rate, the temperature rise time of the lower cap, from baseline to peak, gave an idea about the rapidity of the reaction mechanism. In this respect, the tests where activated primer pellets were employed, systematically featured a slower heat transfer to the container and, thus, a slower heat release. This behavior could be useful for the tuning of the heat release profile.

VII. Conclusion

This work experimentally characterized the heat exchange mechanism between a thermite charge and the container where it was lodged, in both open and closed configuration. The activity focused on iron oxide / aluminum thermites and discarded molybdenum oxide from the tests due to toxicity concerns, still to be confirmed by dedicated chemical analyses.

The work demonstrated that thermite mixtures containing a blend of standard micrometric and activated thermites can react to a thermal stimulus and can transfer a consistent fraction of their reaction enthalpy to the container where they are enclosed. Activated thermites also showed the possibility to act as a temperature-controlled primer for the whole charge, without any external ignition device. The reported case study showed a reaction temperature of about 550 °C. The accuracy of the ignition instant has still to be clearly assessed and requires careful consideration in the light of the correct timing inside a reentry mission profile. An important aspect introduced by thermite mechanical activation is the tunability of the triggering temperature range, thanks to the flexibility introduced by the processing of the primer charge. This capability is very useful for a D4D application since it gives the opportunity to decide the enthalpy release profile of the charge. Moreover, the relatively high threshold needed for ignition is plentifully outside the operating range of spacecraft components, preventing from undue triggering of the demise action.

In the next step of the SPADEXO project these materials will be tested in a hypersonic wind tunnel. The activity will verify if the results obtained in a non-relevant configuration are also achieved for a simulated demise action in a relevant test configuration. Larger thermite charges will be used, and the distribution of primer pellets may be important to grant uniform ignition. In addition, it will be important to verify whether the entrainment effect of gas products and wind tunnel flow on unreacted thermites will produce severe consequences on heat transfer efficiency, once the aerothermal heating breaches the mockup walls during tests. Finally, we should note that for the most part, thermite products are refractory oxides (i.e. alumina) and metals (i.e. iron). These materials can be difficult to demise and may become an additional source of risk for on-ground safety. Although, it is important to underline that such problem arises only if the resulting fragments from thermite reaction overcome the threshold impact energy of 15 J and, in case, specific design configurations may be adopted to circumvent the problem. In the perspective of real D4D application, adequate considerations and tests should be implemented to make thermites an effective, simple, and safe technical solution for an innovative and sustainable demise methodology of large satellites.

Acknowledgments

The authors acknowledge the financial support of the SPADEXO project by the European Space Agency through the Contract No. 4000136082/21/NL/MG.

References

[1] Anon., “Space Debris Mitigation Policy for Agency Projects”, ESA/ADMIN/IPOL(2014)2, ESA Director General’s Office, 2014

[2] AA.VV. “Space Systems - Space Debris Mitigation Requirements”, ISO 24113:2019, *International Organization for Standardization*, BSI Standards Publication.

[3] S. Perrault, T. Soares, and L. Innocenti. "Re-entry Strategies to Comply with Space Debris Mitigation Guidelines", *1st International Obrital Debris Conference*, 9-12 December 2019, Sugar Land (TX), USA.
[4] C. Pardini and L. Anselmo, "The Kinetic Casualty Risk of Uncontrolled Re-entries Before and After the Transition to Small Satellites and Mega-constellations", *Journal of Space Safety Engineering*, Vol. 9, pp. 414-426, 2022.
[5] ESA Space Debris Office, *ESA's Space Environmental Report*, Ref. GEN-DB-LOG-00288-OPS-SD, ESA-ESOC, Issue 6, 2022.
[6] AA.VV. "DIVE – Demise Verification Guidelines for Analysing and Testing the Demise of Man-made Space Objects During Re-entry", *Technical Note*, European Space Agency, 2020.
[7] Cattani, B.M., et al. "An Overview of Deign-for-Demise Technologies", *8th European Conference on Space Debris*, 20-23 April, 2021, Darmstadt, Germany
[8] Dilhan, D., and Omaly, P, "Element de Vehicule Spatial a Capacite d'Autodestruction Amelioree et Procede de Fabrication d'un Tel Element", *Patent FR2975080B1*, filing year 2011.
[9] Seiler, R., and Smet, G., "Exothermic Reaction Aided Spacecraft Demise During Re-entry", *Patent EP3604143A1*, filing year 2018.
[10] Monogarov, K.A., Melnikov, I.N., Drozdov, et al. "Pyrotechnic Approach to Space Debris Destruction: from Thermal Modeling to Hypersonic Wind Tunnel Tests". *Acta Astronautica*, Vol. 172, pp. 47-55, 2020.
[11] Fischer, S.H., and Grubelich, N.C., "Theoretical Energy Release of Thermites, Intermetallics, and Combustible Metals", *24th International Pyrotechnics Seminar*, Monterey, CA. July 1998.
[12] Crane, C., Pantoya, M.L., Dunn, J., "Infrared Measurements of Energy Transfer from Energetic Materials to Steel Substrates*", International Journal of Thermal Sciences*, Vol. 49, 2010, pp. 1877-1885.
[13] Carter, G. Jr., "Portable Metal cutting Pyrotechnic Torch", *US Patent* 2003/0145752A1, filed 5 Feb. 2002.
[14] Weiser, V., Roth, E., Raab, A., del Mar Juez-Lorenzo, M., Kelzenberg, S., Eisenreich, N., "Thermite Type Reactions of Different Metals with Iron-Oxide and the Influence of Pressure", *Propellants Explosives and Pyrotechnics*, Vol. 35, 2010, pp. 240-247.
[15] Tabereaux, A.T., Peterson, R.D., "Aluminum Production", *Treatise on Process Metallurgy, Volume 3: Industrial Processes*, edited by S. Seetharaman, Chap. 2.5, Elsevier, 2014, pp. 839-917.
[16] Glassman, I., Sawyer, S.F., *The Performance of Chemical Propellants*, AGARDograph Vol. 129, Technivision Services, UK, 1970.
[17] Grapes, M.D., et al. "In Situ Observations of Reacting Al/Fe_2O_3 Thermite: Relating Dynamic Particle Size to Macroscopic Burn Time", *Combustion and Flame*, Vol. 201 pp:252–263, 2019.
[18] Pantoya, M.L., Levitas, V.I., Granier, J.J., Henderson, J.B., "Effect of Bulk Density on Reaction Propagation in Nanothermites and Micron Thermites", *Journal of Propulsion and Power*, 25(2), 2009, pp. 465-470.
[19] Granier, J.J., Pantoya, M.L., "Laser ignition of nanocomposite thermites", *Combustion and Flame*, Vol. 138, pp. 373-383, 2004.
[20] Dossi, S., Paravan, C., Maggi, F., Galfetti, L., "Enhancing Micrometric Aluminum Reactivity by Mechanical Activation", *Innovative Energetic Materials: Properties, Combustion Performance and Application*, edited by Pang, W., DeLuca, L., Gromov, A., Cumming, A., Springer, Singapore, 2020, pp. 17-41.
[21] Suryanarayana, C., "Mechanical Alloying and Milling," *Progress in Materials Science*, Vol. 46, 2001, pp.1-184.
[22] Sippel, T.R., Son, S.F., Groven, L.J., "Altering Reactivity of Aluminum with Selective Inclusion of Polytetrafluoroethylene trough Mechanical Activation," *Propellants, Explosives, Pyrotechnics*, Vol. 38, 2013, pp. 286-295.
[23] Y.S. Touloukian and E.H. Buyko, *Thermophysical Properties of Matter - The TPRC Data Series - Vol.4. Specific Heat - Metallic Elements and Alloys*, Purdue University, 1971.